Journal of Engineering Physics and Thermophysics, Vol. 73, No. 1, 2000

THEORETICAL MODELING OF SYSTEMS OF COMBINED THERMAL PROTECTION

A. P. Kuryachii

UDC 532.516+536.423.1

Based on a numerical solution of conjugate boundary problems that describe the processes of heat and mass transfer in two systems of thermal protection of the radiation-evaporation type, the efficiencies of these systems are compared.

Introduction. The principle of operation of systems of combined thermal protection (SCTPs) was proposed for the first time in [1]. The currently developed SCTPs are meant for protection of promising aircraft against intense and prolonged aerodynamic heating. The basic element of the systems considered below is the external heat-resistant shield that takes up intense aerodynamic loads and is overlain by the layer of high-temperature heat insulation and the layer of material saturated with a coolant (water) and mounted on the outer surface of the protected structure.

In developing SCTPs, the creation of mathematical models that describe rather complex processes of heat and mass transfer in different parts of the systems under consideration is of significance. This theoretical modeling makes it possible to evaluate the effect of the basic parameters of the systems on their overall-dimension-weight characteristics and to optimize on this basis the required experimental investigations [2]. The radiation-evaporation method of thermal protection can be realized in systems that are different in structural complexity and efficiency [1-4]. In this work, consideration is given to two combined systems of thermal protection, whose schematic diagrams are described below.

Diagrammatic Representation of an SCTP. It is assumed that the structure protected against external heating has the shape of a plane plate with the thickness h_w, and the density and specific heat of material ρ_w and c_w. The layer of coolant-saturated material is arranged on the outer surface of the plate. Consideration is given to the individual segment of the thermal protection system of the total length $2L$, at the center of which is the origin of the Cartesian coordinate system with the x axis perpendicular to the plate and directed toward the external heat flux. Since the heat and mass transfer and phase transitions in the coolant carrier are not considered in the present formulation of the problem, the origin of the x axis is located on the outer surface of the coolant carrier, which is considered to be the evaporation surface as shown in Fig. 1.

The inner surface of a plane layer of porous heat insulation is at the distance x_1 from the evaporation surface. The thickness of this layer is equal to $h_i = x_2 - x_1$, where x_2 is the coordinate of its outer surface. A thermally thin external plane shield is arranged at the distance x_3 from the evaporation surface. This shield is produced of heat-resistant material and serves to protect the porous heat-insulation layer against intense aerodynamic loads. The unsteady external heat flux $q_e(t)$ arrives at the shield. In the SCTP, just as in passive radiation thermal protection, the major portion of the heat flux $q_e(t)$ is reflected into the ambient medium by the radiation from the surface of the shield heated to a high temperature $T_e(t)$. Unlike the passive system, the portion of the external heat flux that penetrates through the heat-insulation layer is expended mainly on the phase transitions of the coolant.

In the first system under consideration shown in Fig. 1a, a thin sheet reflector that ensures gastightness of the porous layer and a high heat resistance of the gap $0 \le x \le x_1$ due to the small emittances of the reflector surface ε_s is mounted on the inner surface of the insulation layer. The coolant evaporates into a plane channel

N. E. Zhukovskii Central Aerohydrodynamics Institute, Zhukovskii, Russia. Translated from Inzhenerno-Fizicheskii Zhurnal, Vol. 73, No. 1, pp. 44-51, January–February, 2000. Original article submitted May 25, 1999.

1062-0125/2000/7301-0041$25.00

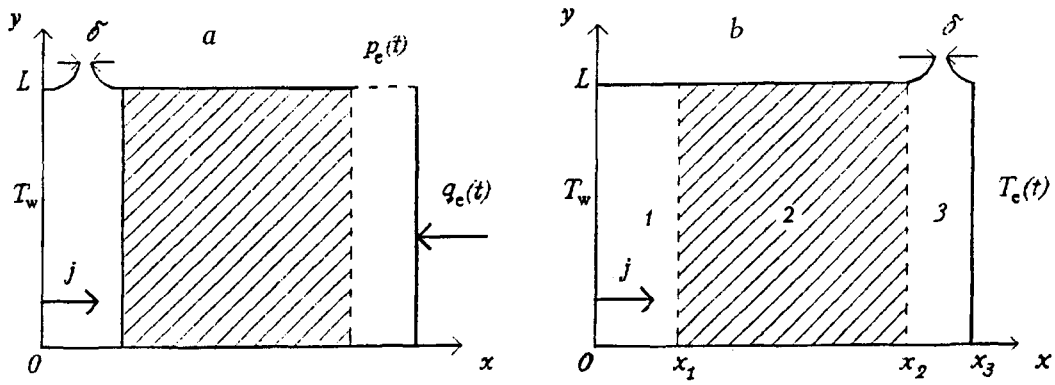

Fig. 1. Schematic diagrams of thermal protection systems: a) with the internal sheet reflector (system 1); b) with a vaportight layer of heat insulation (system 2).

formed by this sheet reflector and an open surface of the coolant carrier. The channel has the axis of symmetry at $y = 0$. Both ends of the channel converge, terminating in slits of width δ that model the real drainage system of the SCTP. The vapor flows out of the channel into the ambient medium with the pressure $p_e(t)$. In the second variant of the SCTP shown in Fig. 1b, the internal sheet reflector is absent. The coolant vapor flows through the porous layer of heat insulation into the channel between this layer and the external heat-resistant shield, then flows outward. Below, the first variant of the combined system of thermal protection will be referred to as system 1, while the second variant will be called system 2.

Formulation of the Problem of Heat and Mass Transfer. In the present work, we consider as a high-temperature heat insulation a slab of superthin quartz fiber with density ρ_i, specific heat c_i, and effective thermal conductivity λ_i that includes all three components of heat transfer: the heat conduction of a solid matrix, the radiation of a porous medium, and the heat conduction of a gas with the prescribed external pressure. Radiation heat transfer in semitransparent thermal protective materials can be evaluated with a sufficient degree of accuracy in the Rosseland approximation. The heat conduction of the gas can be approximated with the aim of allowing for its dependence on the pressure, the temperature, and the diameter of the fibers [5]. In modeling system 1, the pressures both in the porous insulation and in the gap between it and the external shield are assumed to be equal to the external pressure. By analogy with [5], use is made of the formulas for the effective thermal conductivity and the specific heat of the quartz slab that are obtained based on interpolation of experimental data:

$$\lambda_i(T_i) = 1.076 \cdot 10^{-2} + 6.109 \cdot 10^{-5}\left(\frac{T_i}{100}\right)^3 + \lambda_g \quad \text{W/(m} \cdot \text{K)},$$

$$\lambda_g = \lambda_a\left[\left(1 + Z\frac{\rho_i}{\rho_{i0}}\right)^{-1} + 2\left(\frac{2}{\xi} - 1\right)\frac{l}{\Delta}\right]^{-1}, \tag{1}$$

$$\lambda_a = 2.1 \cdot 10^{-3}\frac{T_i^{2/3}}{T_i + 122}, \quad \mu_a = 7.2 \cdot 10^{-4}\lambda_a,$$

$$l = 1.255\frac{\mu_a}{\rho_a\sqrt{R_a T_i}}, \quad c_i(T_i) = 32.13 + 1.91T_i - 7.19 \cdot 10^{-4}T_i^2 \quad \text{J/(kg} \cdot \text{K)}.$$

Here T_i is the insulation temperature; λ_a, μ_a, ρ_a, and R_a are the thermal conductivity, dynamic-viscosity factor, density, and gas constant of the air; ρ_{i0} is the density of fiber material; l is the mean free path of the air

molecules; ξ is the accommodation coefficient; Δ is the average pore width. The best agreement with the available experimental data is obtained for the following values of the indicated parameters: ρ_i = 140 kg/m^3, ρ_{i0} = 2650 kg/m^3, ξ = 0.9, Z = 9.5, and $\Delta = 5 \cdot 10^{-5}$ m.

We assume that the heat-insulation condition is fulfulled at $y = \pm L$, and that changes in the external-shield temperature and the ambient pressure along the fragment of the thermal protection system of the length $2L$ can be disregarded. Heat transfer in the insulation layer of system 1 is modeled within the framework of an ordinary heat conduction equation in the one-dimensional approximation with the use of the effective thermal conductivity (1).

Flow in the vapor-discharge channels of both thermal protection systems under consideration is symmetric relative to the line $y = 0$. It is also assumed that the geometric parameters of the systems satisfy the relations

$$\frac{x_3}{L} << 1\,, \quad \left(\frac{\delta}{x_1}\right)^2 << 1\,, \quad \left(\frac{\delta}{x_3 - x_2}\right)^2 << 1\,. \tag{2}$$

When conditions (2) are fulfilled the flow in the vapor-discharge channels is described by the system of Prandtl equations [6]. The characteristic velocity components across and along the channel are evaluated, respectively, by the expressions [4]

$$u^* = \frac{\delta}{L}\sqrt{R_v T^*}\,, \quad v^* = u^* \frac{L}{x_1}\,. \tag{3}$$

Under the assumptions (2) made, the component of the gas velocity v and the pressure gradient along the channel are linear functions of the y coordinate while the remaining parameters of flow in the main approximation are independent of y [7]. The formulation of the problem and the computational method for unsteady flow of a vapor-air mixture when conditions (2) are fulfilled are described in [4] in detail. Here we only note that, to determine the components of the vapor-air mixture velocity, the mass concentration of the air, the pressure, temperature, and density of the mixture, and the second derivative of the pressure along the channel, use is made of the continuity, momentum, energy, and air-diffusion equations and the equation of state of the vapor-air mixture, the condition of equality of the flow rate in the cross section $y = L$ to the flow rate through the drainage slit, and the condition of equality of the vapor pressure on the evaporation surface to the saturation pressure at its temperature. The unsteady conjugate boundary problem of calculating the minimum weight of system 1 for prescribed $q_e(t)$ and $p_e(t)$ is also formulated in [4].

We present below a physical-mathematical model of system 2, whose schematic diagram is shown in Fig. 1b. This variant of thermal protection combines the features of radiation, evaporation, and transpiration systems. Consideration is given to three basic regions of system 2: evaporation cavity (1), porous-insulation layer (2), and vapor-discharge channel (3). The vapor pressure in the indicated regions is denoted subsequently as p_1, p_2, and p_3.

The boundary problem that describes the heat and mass transfer in the evaporation region and the heat insulation is formulated in a one-dimensional approximation. Since the heat capacity of the vapor per unit volume is much lower than in the porous insulation the unsteady term in the energy equation of the gas can be disregarded. It is also assumed that the hydrodynamic relaxation time of the flow $t_u = x_3/u^*$, where the characteristic flow velocity in the insulation u^* is evaluated by expression (3), is small as compared to the characteristic time of heating of the entire system because of the external thermal action. Under these assumptions, vapor flow can be considered in a quasistationary approximation.

The continuity and momentum equations yield that the vapor flux and the pressure are constant across the evaporation cavity. The first is equal to the evaporation rate, while the second is equal to the pressure of saturated vapor at the evaporation-surface temperature. The boundary condition on the evaporation surface given below reflects the fact that heating of the protected structure and evaporation of the coolant are due to

the supply of heat by the heat conduction of the gas phase and the radiation heat transfer between the surfaces of the coolant carrier and the porous insulation that is described within the framework of the model of diffusely gray bodies.

Thus, the heat and mass transfer equations with the corresponding boundary conditions in the evaporation cavity have the following form:

$$\rho_v u = j(t), \quad p_1 = p_{vs}(T_w) = 133.4 \exp\left(18.681 - \frac{4104}{T_w - 35}\right),$$

$$jc_p \frac{dT_v}{dx} = \frac{d}{dx}\left(\lambda_v \frac{dT_v}{dx}\right), \tag{4}$$

$$x = 0: \quad (\rho_w c_w h_w + m_{liq} c_{liq}) \frac{dT_w}{dt} + rj = \lambda_v \frac{dT_v}{dx} + \varepsilon_1 \sigma (T_{i1}^4 - T_w^4),$$

$$\varepsilon_1 = \frac{\varepsilon_w \varepsilon_i}{\varepsilon_w + \varepsilon_i - \varepsilon_w \varepsilon_i}.$$

Here j is the evaporation rate of the coolant; ρ_v, c_p, λ_v, and T_v are the density, specific heat at constant pressure, thermal conductivity, and temperature of the vapor; p_{vs} is the pressure of the saturated vapor; $r = r_0 - (c_{liq} - c_p)T_w$ is the vapor temperature; r_0 is the heat of evaporation at 0° K; c_{liq} and m_{liq} are the specific heat and mass of the liquid coolant per unit area; ε_i and T_{i1} are the emittance and temperature of the heat-insulation surface; ε_w and T_w are the emittance and temperature of the evaporation surface.

Heat and mass transfer in the layer of heat insulation (region 2) is modeled with allowance for the interphase heat transfer and the difference of the vapor and porous-medium temperatures. The continuity equation for region 2 yields that the vapor flux depends only on time. Vapor flow in the insulation is assumed to be slow and therefore is described by the Darcy equation

$$j(t) = -\frac{K}{\mu_v} \rho_v \frac{dp_2}{dx}. \tag{5}$$

Under the assumption that the gas equation is fulfilled for the vapor, as a result of integration of Eq. (5) we find the distribution of the vapor pressure in the porous layer

$$p_2(x, t) = \left(p_1^2 - 2j \frac{R_v}{K} \int_{x_1}^{x} \mu_v T_v dx\right)^{1/2}. \tag{6}$$

The energy equation of the vapor with allowance for the interphase heat transfer has the form

$$jc_{pv} \frac{dT_v}{dx} + s\alpha (T_v - T_i) = \frac{d}{dx}\left(\lambda_v \frac{dT_v}{dx}\right), \tag{7}$$

where s and α are the effective area per unit volume and the coefficient of convective heat transfer of the porous medium.

For simplification, all the quartz fibers that form the porous slab are assumed to have the shape of circular cylinders of constant diameter d and to be perpendicular to the x axis. In this case, the specific area of the inner surface of the porous body is evaluated as $s = 4(1 - \varphi)/d$, where φ is the porosity of the slab.

Convective heat transfer between the gas and the porous matrix is a complex process. To determine the coefficient α, use is usually made of the relationship between the local Nusselt number $\mathrm{Nu} = \alpha d/\lambda_v$ and the

Reynolds number $\mathrm{Re}_d = \rho_v u d/\mu_v$ [8]. In the present work, for evaluation of the effective coefficient of heat transfer we took the correlation equation from [9]

$$\mathrm{Nu} = (0.4\,\mathrm{Re}_d^{1/2} + 0.06\,\mathrm{Re}_d^{2/3})\,\mathrm{Pr}^{2/5}\left[\frac{\mu_v(T_v)}{\mu_v(T_i)}\right]^{1/4}.$$

The energy equation of the heat-insulation layer and the corresponding boundary conditions have the following form:

$$\rho_i c_i \frac{\partial T_i}{\partial t} + s\alpha\,(T_i - T_v) = \frac{\partial}{\partial x}\left(\lambda_i \frac{\partial T_i}{\partial x}\right),$$

$$x = x_1:\ \lambda_i \frac{\partial T_i}{\partial x} = \varepsilon_1 \sigma\,(T_i^4 - T_w^4), \tag{8}$$

$$x = x_2:\ \lambda_i \frac{\partial T_i}{\partial x} = \varepsilon_2 \sigma\,(T_e^4 - T_i^4),\quad \varepsilon_2 = \frac{\varepsilon_i \varepsilon_e}{\varepsilon_i + \varepsilon_e - \varepsilon_i \varepsilon_e},$$

where ε_e is the emittance of the surface of the external shield.

We note that only the radiation heat transfer between the surfaces of the insulation, the coolant carrier, and the external shield enters in the boundary conditions for the energy equation of the insulation (8) since the conductive and convective heat transfers in regions 1 and 3 are determined by the gas phase. The effective thermal conductivity of the insulation employed in solving (8) is determined by Eq. (1) without the last term since the convective heat transfer in region 2 is described by the energy equation of the vapor.

As has been noted above, the longitudinal velocity component and the pressure gradient in the vapor-discharge channel with converging ends can be represented in the form $v = y\omega(t)$ and $\partial p_3/\partial y = yF(t)$. In this case, the energy, continuity, and momentum equations that describe vapor flow in region 3 are represented in a quasistationary approximation as

$$\rho_v u c_p \frac{dT_v}{dx} = \frac{d}{dx}\left(\lambda_v \frac{dT_v}{dx}\right);\quad x = x_3:\ T_v = T_e,$$

$$\rho_v u = j - \int_{x_2}^{x} \rho_v w\,dx;\quad x = x_3:\ u = 0, \tag{9}$$

$$\rho_v u \frac{dw}{dx} + \rho_v w^2 + F = \frac{d}{dx}\left(\mu_v \frac{dw}{dx}\right);\quad x = x_2, x_3:\ w = 0.$$

The condition of equality of the flow rate of the coolant to the flow rate of the vapor through the drainage slit, for which use is made of the formulas of adiabatic escape of the gas from the cavity

$$\Gamma \delta p_3 (R_v \langle T_v \rangle)^{-1/2} Q(\pi) = jL,\quad \Gamma = \left[\gamma\left(\frac{2}{\gamma - 1}\right)^{(\gamma+1)/(\gamma-1)}\right]^{1/2},$$

$$Q(\pi) = 1,\quad \pi \equiv \frac{p_e}{p_3} \le \pi_* = \left(\frac{2}{\gamma + 1}\right)^{\gamma/(\gamma-1)}, \tag{10}$$

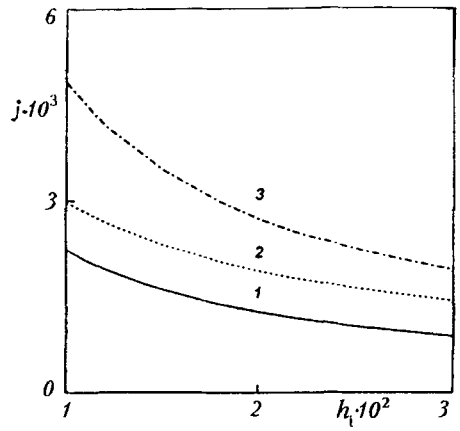

Fig. 2. Evaporation rates of the coolant as functions of heat-insulation thickness: in system 2 (1) and in system 1 for $\varepsilon_s = 0.3$ (3). j, kg/(m^2·sec); h_i, m.

$$Q(\pi) = \left(\frac{\pi}{\pi_*}\right)^{1/\gamma}\left[\frac{\gamma+1}{\gamma-1}\left(1-\pi^{(\gamma-1)/\gamma}\right)\right]^{1/2}, \quad \pi > \pi_*,$$

where $\gamma = 1.3$ is the adiabatic exponent of the water vapor and $\langle T_v \rangle$ is the average vapor temperature across the channel, serves to determine the second derivative of pressure along the channel F.

The transfer coefficients of the vapor are computed by the formulas obtained by numerical interpolation of tabulated data [10]:

$$\lambda_v(T) = (-5.8 + 0.0856T)\cdot 10^{-3} \quad \text{W/(m}\cdot\text{K)},$$

$$\mu_v(T) = (-3.05 + 0.0406T)\cdot 10^{-6} \quad \text{kg/(m}\cdot\text{sec)}.$$

The formulated boundary problem (4)-(10) enables us to calculate the unknown functions of j, p, ρ_v, T_v, T_i, u, w, and F that describe the processes of heat and mass transfer in the system of thermal protection under consideration.

It is necessary to note that in modeling actual thermal actions on the aircraft the situation where the initial total pressure of the air and the vapor in the thermal protection system that is equal to the external pressure will exceed the pressure of saturated vapor at the initial temperature of the system, i.e., $p_0 > p_{vs}(T_0)$, will be typical. The analysis of flow of a vapor-air mixture in a vapor-discharge channel made in [4] shows that as long as the air is present in the channel the evaporation rate is much lower than its value on removing completely the air from the channel. Therefore when the external thermal action is rather prolonged we can disregard the total flow rate of the coolant during the initial stage of heating of the thermal protection system.

On this basis, it is assumed in the model proposed that as long as the external pressure exceeds the pressure of saturated vapor at the evaporation-surface temperature during the unsteady stage of heating the pressure in all parts of the system is equal to the external pressure and the evaporation rate is zero. This assumption holds true until the evaporation-surface temperature attains the value at which the condition $p_{vs}(T_w) \geq p_e(t)$ is fulfilled. From this point on, problem (4)-(10) is solved without any additional simplifications.

Comparison of Thermal Protection Systems. Based on the models presented above and in [4] we calculated the heat and mass transfer in the systems under consideration for the following fixed values of the parameters: $L = 0.5$ m, $x_1 = 0.01$ m, $x_3 - x_2 = 0.005$ m, $\delta = 5\cdot 10^{-5}$ m, $h_w = 0.002$ m, $\rho_w = 2800$ kg/m^3, $c_w = 900$ J/(kg·K), $\varepsilon_{e,i,w} = 0.8$, $\varphi = 0.9$, $K = 10^{-12}$ m^2, and $d = 2\cdot 10^{-4}$ m. The temperature of the external shield and the ambient pressure varied linearly with time from the initial values $T_0 = 290$ K and $p_0 = 10^5$ Pa to the limiting values $T_{e\,max} = 1500$ K and $p_{e\,min} = 500$ Pa and thereafter remained constant.

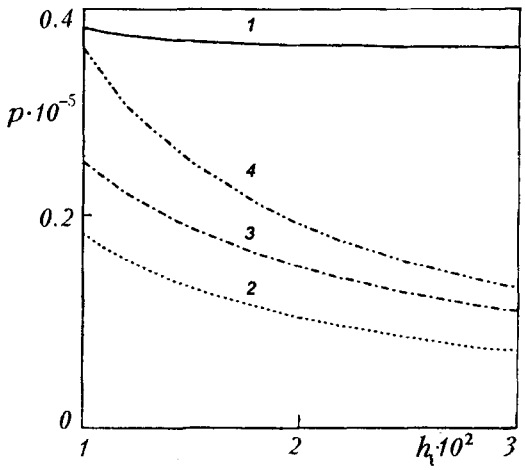

Fig. 3. Pressures in the evaporation cavity (1) and the external channel (2) of system 2 and in the vapor-discharge channel of system 1 as functions of heat-insulation thickness for $\varepsilon_s = 0.1$ (3) and $\varepsilon_s = 0.8$ (4). p, Pa.

Figure 2 presents the steady-state evaporation rates of the coolant as functions of the thickness of the insulation layer. Here curve 1 corresponds to system 2, curve 2 presents the results for system 1, in which the emittance of the internal sheet reflector is $\varepsilon_s = 0.1$, and curve 3 corresponds to $\varepsilon_s = 0.8$. The substantially lower flow rate of the coolant in system 2 is associated with the use of the principle of a transpiration system. In heating the vapor to the external-shield temperature, the heat capacity of the vapor is used in addition to the heat of evaporation of the coolant. Figure 2 also shows a significant effect of the emittance of the sheet reflector in system 1. Interestingly, the ratio of the evaporation rates j_2/j_1 (system 2/system 1) is nearly constant and is equal to 0.46 in the considered range of variation in the slab thickness for a high emittance of the sheet reflector $\varepsilon_s = 0.8$ in system 1. When $\varepsilon_s = 0.1$ this ratio decreases as the slab thickness decreases: $j_2/j_1 = 0.75$, 0.66, and 0.61 for $h_i = 1$, 2, and 3 cm, respectively, i.e., the efficiency of system 2, as compared to system 1, increases with insulation thickness.

We note that the minimum total weight of the radiation-evaporation thermal protection $m_t \approx \rho_i h_i + j\Delta t$ (where Δt is the duration of the thermal action) is attained when the masses of the insulation layer $m_i = \rho_i h_i$ and the initial supply of the coolant $m_{liq0} \approx j\Delta t$ are approximately equal [3, 4]. It follows that the ratio of the minimum masses of the systems under consideration is evaluated from the ratio of the evaporation rates of the coolant in them.

Another important parameter of the systems of combined thermal protection is the pressure difference on the insulation layer. For concrete thermal protective materials and concrete regimes of flight of the aircraft, this parameter can turn out to be a limiting factor of the maximum permissible insulation thickness in optimizing the overall dimension and weight of the system under consideration. The effect of the heat-insulation thickness on the levels of steady-state pressure in the cavities of the considered systems is shown in Fig. 3. Here curves 1 and 2 present the pressure in the evaporation cavity and the external channel of system 2, while curves 3 and 4 present the pressure in the vapor-discharge channel of system 1 for the emittances of the sheet reflector $\varepsilon_s = 0.1$ and 0.8, respectively.

With the prescribed temperature of the external shield and ratio δ/L in both systems of combined thermal protection the pressure in the vapor-discharge channel is governed by the evaporation rate related to the vapor flow rate through drainage slits. Therefore the pressure difference on the insulation layer decreases as its thickness increases in system 1 (the pressure in the gap between the insulation layer and the external shield is equal to the external pressure). In system 2, in spite of the strong dependence of the evaporation rate (and the pressure in the external channel) on the slab thickness, the pressure of saturated vapor in the evaporation cavity changes slightly because of the small temperature change of the evaporation surface. Therefore the pressure

decrease in the external channel as a result of the increase in the slab thickness leads to an increase in the pressure difference on the insulation layer.

Conclusion. The mathematical models of combined systems of thermal protection proposed make it possible to calculate their basic characteristics, in particular, the temperature distributions, the evaporation rate of the coolant, and the pressure difference on the insulation layer. It is shown that the system of thermal protection, in which use is made of filtration of the coolant vapor through the layer of heat insulation, is more efficient than the system with a vaportight insulation layer.

The work was carried out with financial support from the Russian Fund for Fundamental Research (grant No. 96-15-96063 of support of the leading scientific schools).

NOTATION

T, temperature; q, heat flux; t, time; j, vapor flux; ρ, density; p, pressure; c, specific heat; λ, thermal conductivity; μ, dynamic-viscosity factor; R, gas constant; r, specific heat of evaporation; ε, emittance; σ, Stefan-Boltzmann constant; x and y, coordinates; u and v, velocity components; w, longitudinal gradient of the vapor velocity directed along the vapor-discharge channel; K, permittivity; d, fiber diameter; δ, drainage-slit width; L, half-length of the segment of heat insulation; Nu, Nusselt number; Re, Reynolds number; Pr, Prandtl number. Subscripts: v, vapor; i, heat insulation; w, evaporation surface; e, external medium; s, shield; g, gas; vs, saturafed vapor.

REFERENCES

1. L. Roberts, *Advances in Aeronautics Sci.*, New York, **4**, 1019-1044 (1962).
2. I. N. Bobrov and A. P. Kuryachii, *Teplofiz. Vys. Temp.*, **34**, No. 1, 75-82 (1996).
3. J. H. Bridges and F. D. Richmond, in: *Technol. Lunar Explorat.*, New York–London (1963), pp. 761-782.
4. A. P. Kuryachii, *Izv. Ross. Akad. Nauk, Mekh. Zhidk. Gaza*, No. 1, 24-36 (1985).
5. W.-D. Ebeling, W. P. P. Fisher, J. Antonenko, and L. Paderin, *SAE Technical Paper*, Series No. 951577, 1-9 (1995).
6. J. C. Williams, *AIAA J.*, **1**, 185-195 (1963).
7. H. van Ooijen and C. J. Hoogendoorn, *AIAA J.*, **17**, No. 11, 1251-1259 (1979).
8. S. Maruyama and R. Viskanta, *AIAA Paper*, No. 605, 1-11 (1989).
9. S. Whitaker, *AIChE J.*, **18**, No. 2, 361-370 (1972).
10. M. P. Vukalovich, *Thermophysical Properties of Water and Water Vapor* [in Russian], Moscow (1967).